Advances in Science and Technology Research Journal

Advances in Science and Technology Research Journal, 2025, 19(8), 345–358
https://doi.org/10.12913/22998624/205716
ISSN 2299-8624, License CC-BY 4.0

Received: 2025.05.03
Accepted: 2025.06.15
Published: 2025.07.01

Optimization of fused deposition modeling parameters to enhance tensile strength and surface roughness of polyethylene terephthalate glycol

Alaa Hassan Shabeeb[1*], Ahmed Basil Abdulwahhab[1], Hameed S. Ismael[2], Safaa Kadhim Ghazi[1]

[1] Department of Production Engineering and Metallurgy, University of Technology, Baghdad, Iraq
[2] Civil Engineering, University of Technology, Baghdad, Iraq
* Corresponding author's e-mail: safaa.kadhim1988@gmail.com

ABSTRACT

The wide examination of fused deposition modeling (FDM) as an industrial additive manufacturing technique appears because it provides design freedom alongside improved material efficiency and reasonable cost. This study's main objective is to investigate the relationship of FDM process parameters with the tensile properties and surface roughness of polyethylene terephthalate glycol (PETG) parts. A response surface methodology (RSM) utilizing Box-Behnken design methodology studied three essential parameters consisting of infill density and layer height, together with plate temperature. The analysis demonstrated that layer height proved to be the main element affecting tensile strength because it contributed 80.9% of the experimental variations, while infill density stood out as the leading determinant of surface roughness, which was responsible for 78% of the contribution. Experimental testing proved that the predictive model showed accurate results when validated through measurements of tensile strength, which produced maximum errors of 1.28%, and surface roughness, which yielded maximum errors of 6.54%. A desirability analysis indicated that the ideal parameters of the roughness and tensile strength of the printed parts included an infill density of 64.24% combined with a layer height of 0.1813 mm and plate temperature of 51.46 °C. These outcomes provide a comprehensive understanding of process parameter effects that result in quality PETG parts with mechanical performance. The two-axis optimization methodology for PETG also enhances its use in functional engineering systems that require simultaneous mechanical durability and manufacturing accuracy.

Keywords: polyethylene terephthalate glycol, FDM, process parameters, tensile strength, surface roughness.

INTRODUCTION

Fused deposition modeling (FDM) classification represents a well-known additive manufacturing process that produces components through successive buildup of heated thermoplastic filaments emerging from a nozzle [1]. The process requires different thermoplastic materials, including polylactic acid (PLA), acrylonitrile butadiene styrene (ABS), and polyethylene terephthalate glycol (PETG), to deposit sequential layers on the platform until proper solidification occurs. FDM features affordability alongside design adaptability and detailed production capabilities which render it appropriate for multiple purposes across industrial fields and creative activities, including initial design phases as well as operational applications [2].

Multiple elements that include printing parameters material selection, and post-processing practices determine the achievement of high-quality end products in FDM printing systems. FDM printing technology leads to component characteristics that stem from different processing parameters such as layer thickness, printing speed, temperature, fill density, and nozzle diameter. The material's tensile strength, along with surface roughness dimensional accuracy, and porosity values, depend on the printing parameters [3, 4]. Material behavior during printing heats produces the strength of layer bonds, which ultimately decides product quality levels.

Several studies show that various FDM printing parameters influence both the strength of produced parts and their surface quality [5]. The tensile strength and surface texture of printed products depend on three main factors: size, thickness, and deposition speed, together with extrusion temperature specifications as well as material density and orientation angle values. Interlayer bond strength increases with reduced voids when printers use thinner print layers [6]. The denser the infill density becomes, the better the mechanical properties develop since structures with few defects exhibit superior strength and durability [7].

The mechanical properties, together with the surface finish, are strongly affected by how hot manufacturers set the extrusion temperature. The surface quality improves because heat lowers material viscosity yet raises the risk of filament failure and deformation at elevated temperatures. Building platforms require an optimal temperature to ensure first-layer adhesion because it stops defects like warping and delamination from appearing. The structural properties of printed layers, together with surface quality, receive their defining qualities based on how the height value affects attributes in exactly the opposite way [8, 9].

Studies have extensively analyzed the connection between machine parameters and the mechanical characteristics of FDM-produced components with an emphasis on strength properties and product surface conditions. The parameters play an essential role in enhancing mechanical performance and satisfying design criteria about structural strength together with functional usability of printed components, Mohd et al. [9] this study evaluated the effect of the annealing process on improving the tensile strength and surface quality of 3D-printed ABS parts. Annealing temperatures between 120 and 180 °C were used, with annealing periods ranging from 20 to 60 minutes. The sample treated at 120 °C/20 minutes achieved the lowest surface roughness (0.622 μm) and the highest tensile strength (75.681 MPa), while the sample treated at 180 °C/60 minutes achieved the maximum surface roughness (3.246 μm). The samples achieved their best strength at 180 °C during a 60-minute annealing process, and the results indicated a significant difference between the surface finish quality of the annealed-treated ABS and the mechanical performance results. A study by Farashi et al. [10] evaluated the printing process variable relationships with mechanical characteristics of FDM-created samples through studies of layer dimensions and orientation choices. Results showed that layer thickness enhancement leads to a maximum 20% reduction in tensile strength in addition to decreased mechanical properties by about 12% when tilting the printing angle with higher extruder temperatures and lower printing speeds. In another work, Lalegani et al. [11] analyzed how the filler pattern, along with density levels, affected the surface roughness and tensile strength measurements of PLA products produced by combining computer-aided design (CAD) and fused deposition modeling. four filler patterns – grid, triangular, zigzag, and concentric were u sed. Results indicated that the concentration arrangements produced both the smoothest surface condition and the best tensile strength using either method. Shirmohammadi et al. [12] developed a technique that combines artificial neural networks and particle swarm algorithms to improve surface roughness results for FDM 3D printing. They used a central composite design to generate 43 experiments to study five independent parameters, including nozzle temperature, layer thickness, printing speed, nozzle diameter, and material density. Results showed an optimized additive manufacturing process operated at 192.20 °C nozzle temperature, 100 μm layer thickness, and printing at 97.06 mm/s speed with 0.3 mm nozzle diameter, which delivered 24.88% material density and produced an 11.319 μm surface finish. Mat et al. [13] focused on assessing the influence of environmental parameters on dimensions in fused filament fabrication (FFF) printed components. This research utilized acrylonitrile butadiene styrene material as it worked with different layer dimensions (0.1 mm, 0.2 mm, and 0.3 mm) while using nitrogen gas to reduce oxygen content in the printer chamber. The study utilized laboratory testing to measure tensile strength as well as surface roughness parameters for assessing how oxygen content affected printed object quality. Results showed maximum tensile strength reached 11.767 MPa in the tests. Mani et al. [14] explored ways to optimize the parameters of the fused deposition modeling 3D printing process to improve product quality standards. Three parameter settings were used at three levels to produce polylactic acid samples conforming to ASTM requirements by adjusting the layer dimensions, nozzle temperature, and test densities. An orthogonal matrix was generated using the Taguchi design process for these parameters. Surface roughness tests, as well as tensile and hardness measurements, were performed. Analysis revealed that the optimal conditions for delivering tensile strength consisted of using a 0.35 mm layer thickness and 65% fill density at a nozzle temperature of 220 °C. In comparison, the best parameters for producing hardness were a 0.25 mm layer thickness and 65% fill density at a nozzle temperature of 215 °C. The required surface roughness was a 0.15 mm layer thickness and 55% fill density at a nozzle temperature of 210 °C. Abdulridha et al. [15] focused on the effect of FDM process variables on the mechanical and physical PLA samples. Six crucial production parameters were investigated, which consisted of packing pattern along with packing density, overlap ratio, layer thickness and shell thickness, and the number of upper as well as lower layers. The test results confirmed that the maximum tensile strength of 55 MPa came from using 80% packing density, together with 0.25 mm layer thickness, and 0.8 mm shell thickness, along with six upper/lower layers and a 10% packing overlap. Necmettin et al. [16] focused on the effects of the mechanical and physical properties of PLA, PETG, and ABS materials produced on tensile strength, hardness, surface roughness, and water absorption tests were used to compare the behavior of these thermoplastics. The study revealed that PETG experienced the highest tensile stress, while ABS and PLA exhibited lower values. The tests showed that PETG was the stiffest, while PLA and ABS recorded lower values. Our analysis found that ABS had the roughest surface without sanding, but sanding improved the smoothness of all samples. A large number of researchers have looked in depth at how FDM parameters impact part strength and surface quality, but optimizing these parameters for PETG has not been widely explored. Many applaud PETG for being both strong and flexible, as well as durable and resistant to chemicals, and great where a strong and attractive finish is desirable. There has been only limited research done so far on how FDM parameters shape both the strength and smoothness of PETG.

This study examined the complete optimization of FDM parameters, which control the production of polyethylene terephthalate glycol components through the study of infill density, layer height, and plate temperature. Applying sophisticated experimental design and statistical methods, the research used the Response Surface method alongside desirability function approaches to optimize multiple performance metrics while systematically considering strength and surface quality. This research tries to uncover relationships between main process variables and main performance indicators for PETG. The new aspect of this study is that it sets out in an organized way to tune FDM process parameters for PETG and maximizes both the tensile strength and the looks of finished parts.

METHODOLOGY

Material and method

The ANYCUBIC 3D printer executed the experimental tasks based on Figure 1. The research material consisted of a grey PETG filament, which had a diameter of 1.75 mm because it represents a popular choice for 3D printing applications due to its easy usage as well as durable mechanical features, and green nature. PETG proves an exceptional filament for making prototypes and production items, which span from consumer items through architectural creations to educational models. The material provides both excellent interlayer bonding and high stiffness properties and moderate tensile strengths, together with low dimensional changes [17, 18]. Distribution of PETG starting materials from renewable sources, along with its biodegradable nature, makes it a perfect choice for environmentally friendly applications. The performance of PETG is limited compared with PLA and ABS because of these filaments [19]. PETG offers reduced durability against heat exposure from extreme temperatures while maintaining brittleness as its main weakness for applications that need resilient flexibility. Surface roughness represents a well-recognized difficulty in PETG printing because the printed surface finish closely relates to the inputted printing parameters, including layer height plate temperature, and infill density. Surface roughness at a high level will negatively impact the quality of both the external appearance and the dimensions of printed parts, particularly in intricate designs or big models [20]. Despite these challenges, PETG remains one of the most popular filaments in 3D printing due to its versatility, accessibility,

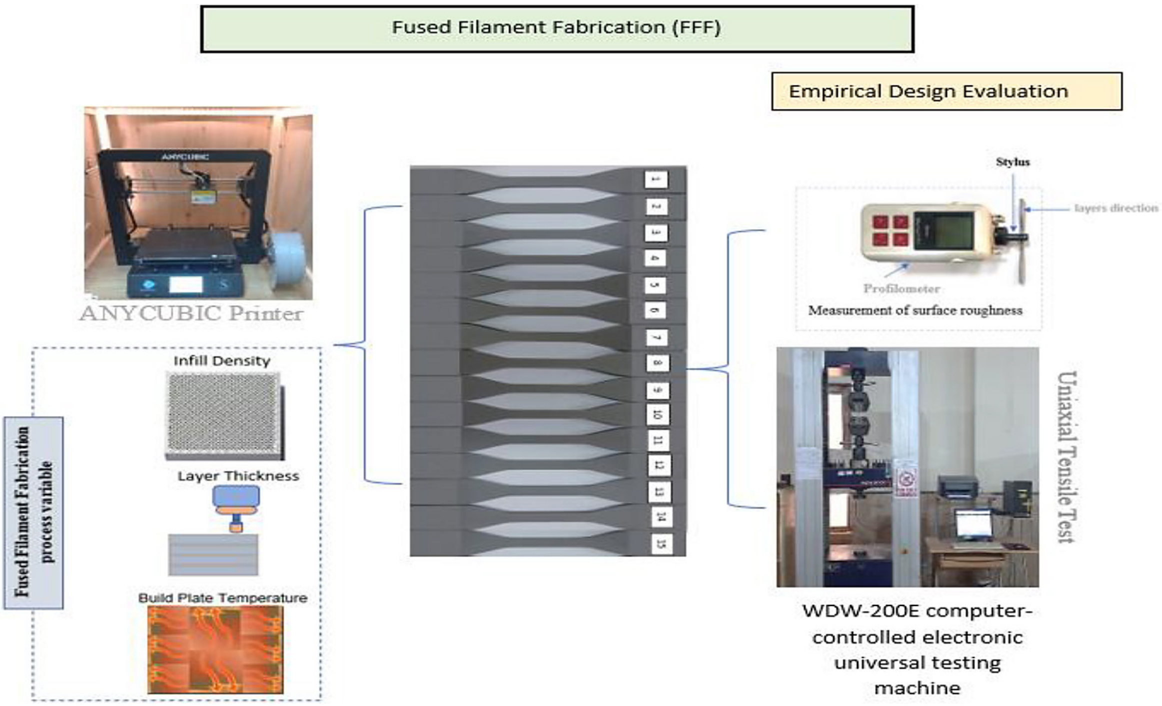

Figure 1. Printing process and measurements.

and ability to produce surface-stable parts with minimal warping.

The standard triangle language (STL) file created by Solidworks was transformed by the Cura 4.13.1 to G code, which the machine can read to print. Figure 2 a,b, depicts the solid model and sliced model used by the ASTM D638 Type 4 standards. Table 1 lists the levels of three input parameters used to fabricate the PETG filament to be used in this study. All the experiments here use the same fixed FDM parameters as listed in Table 2.

The production of the specimens was carried out using the Box-Behnken methodology, where 15 runs (replicates) are required in the response surface method (RSM) [21]. The input parameter pairs have been coded as A, B, and C, respectively, with their varying levels outlined in Table 3. For DOE and statistical analysis, Minitab 17 software was used [22]. This tool allowed for the evaluation and optimization of process parameters to obtain reliable results. The complete workflow, from selecting FDM parameters to implementing optimization techniques, is illustrated in Figure 3.

The mechanical properties of the fabricated PETG specimens were evaluated through tensile testing carried out on a WDW200E computer-controlled electronic universal testing machine; tensile testing of the fabricated specimens was conducted on a WDW200E computer-controlled electronic universal measuring machine by ASTM D638 Type IV standards [23, 24] as shown in Figure 1. Testing was carried out at room temperature with a constant crosshead speed of 1.5 mm/min, and the three modes of data (load, deformation, stroke, and time) were continuously recorded. The peak load values taken from recorded data and corresponding with precise measurements of

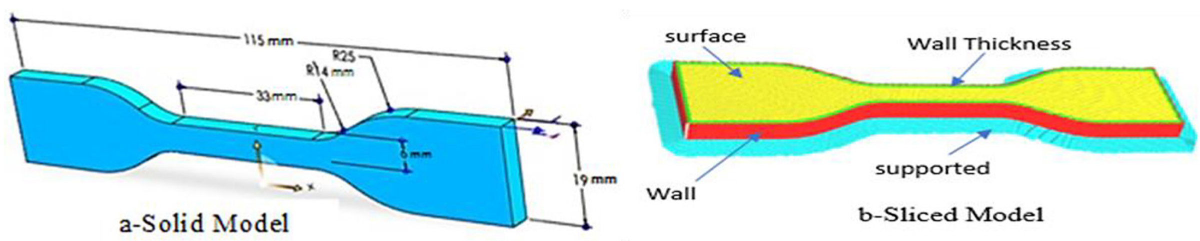

Figure 2. Solid and sliced models for tensile specimens

Table 1. 3D printing parameters and their levels

FDM parameters	Units	Levels		
		1	2	3
Infill density	%	40	60	80
Layer height	(mm)	0.15	0.20	0.25
Plate temperature	°C	45	50	55

Table 2. Fixed parameters

Parameter type	Values	Units
Wall thickness	1.2	mm
Printing speed	55	mm/s
Infill pattern	Line	-

each specimen's actual dimensions (rather than CAD model parameters) were used for calculation with the peak load values to provide the ultimate tensile strength. These experimental measurements served to determine stress values and mechanical properties as well as to estimate the tensile strength of each PETG test sample using Equation 1.

$$\sigma = \frac{F}{A} \tag{1}$$

where: σ – tensile stress (N/mm^2); F – applied force (N); A – cross section area (mm^2).

In this work, tensile test sample surface roughness was evaluated using the Pocket Surf profile measurement device, as shown in Figure 1. The Ra parameter was calculated three times for each specimen by three measurements of the roughness perpendicular to the orientation of the layer at 3 different places on the sample to obtain a roughness value. Finally, these three measurements were averaged to give the final measured surface roughness value for each printed part.

RESULTS AND DISCUSSION

The gathering of data for tensile strength and surface roughness from PETG samples appears in Table 4 and is presented visually in Figures 4 and 5 through bar charts. Experimental tensile strength increased from 40.013 MPa to 44.666 MPa with a 40% infill density (level 1) paired with a 0.20 mm layer height (level 2) and a 45 °C plate temperature (level 1). This is significant as it exceeds the 28.53 MPa maximum expected tensile strength reported in reference [25]. The combination of an infill density at level 2, a layer height at level 2, and a plate temperature at level 2 produced a specimen with surface roughness values decreasing sharply from 9.560 µm to 6.130 µm. The study demonstrates how specific process variables affect the simultaneous enhancement of PETG-based 3D printing mechanical outcomes and printing surface quality.

Using the RSM technique in MINITAB 17, Analysis of Variance (ANOVA) was used to evaluate how tensile strength and surface roughness changed concerning input parameters. A P-value of less than 0.05, or a 95% confidence interval, was used as the statistical significance criterion for the analysis, which was based on experimental data described in Table 5. A model term was considered statistically significant if its P-value was less than this threshold.

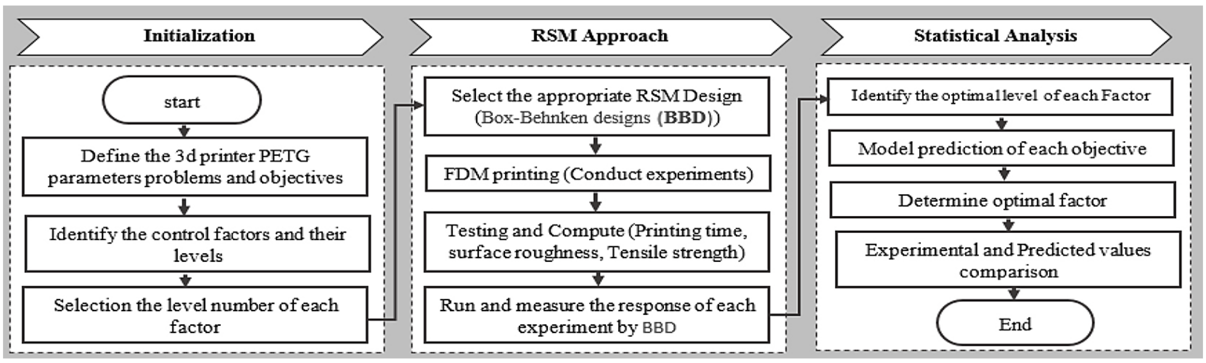

Figure 3. Overview of process parameters optimization and prediction methodology

Table 3. Box-Behnken design's coded and real printer parameter combinations

Exp. No.	Coded parameters			Actual parameters		
	A	B	C	Infill density (%)	Layer height (mm)	Plate temperature (°C)
1	-1	-1	0	40	0.15	50
2	1	-1	0	80	0.15	50
3	-1	1	0	40	0.25	50
4	1	1	0	80	0.25	50
5	-1	0	-1	40	0.20	45
6	1	0	-1	80	0.20	45
7	-1	0	1	40	0.20	55
8	1	0	1	80	0.20	55
9	0	-1	-1	60	0.15	45
10	0	1	-1	60	0.25	45
11	0	-1	1	60	0.15	55
12	0	1	1	60	0.25	55
13	0	0	0	60	0.20	50
14	0	0	0	60	0.20	50
15	0	0	0	60	0.20	50

Table 4. Experimental results for tensile strength and surface roughness

Exp. No.	Infill density (%)	Layer height (mm)	Plate temperature (°C)	Tensile strength (MPa)	Surface roughness (µm)
1	40	0.15	50	41.720	7.590
2	80	0.15	50	43.512	7.066
3	40	0.25	50	41.812	7.640
4	80	0.25	50	41.370	8.350
5	40	0.20	45	44.666	8.310
6	80	0.20	45	41.390	9.560
7	40	0.20	55	42.857	8.680
8	80	0.20	55	44.665	8.830
9	60	0.15	45	41.847	7.860
10	60	0.25	45	40.013	7.980
11	60	0.15	55	42.572	6.730
12	60	0.25	55	41.914	8.150
13	60	0.20	50	43.116	6.460
14	60	0.20	50	43.913	6.980
15	60	0.20	50	43.981	6.130

The outcome showed that layer height significantly influences tensile strength because the P-value reached 0.038. Tensile strength improves when the interlayer cohesion is enhanced through the reduction of layer height. The results and findings showed infill density as the main determinant of surface roughness because its P-value reached 0.010 at the 95% confidence level. The density of infill material determines internal void presence, so print surfaces remain smoother because shrinkage and surface deformation are minimized.

The analysis depicts the influence of infill density together with layer height and plate temperature through Figures 6 and 7 regarding tensile strength and surface roughness measurement. Tensile strength exhibits a substantial enhancement when the layer height decreases abruptly from 0.2 mm to 0.25 mm, according to Figure 6, while Figure 6 also shows that plate temperature elevation from 50 °C to 55 °C leads to a moderate strength gain. The results indicate infill density

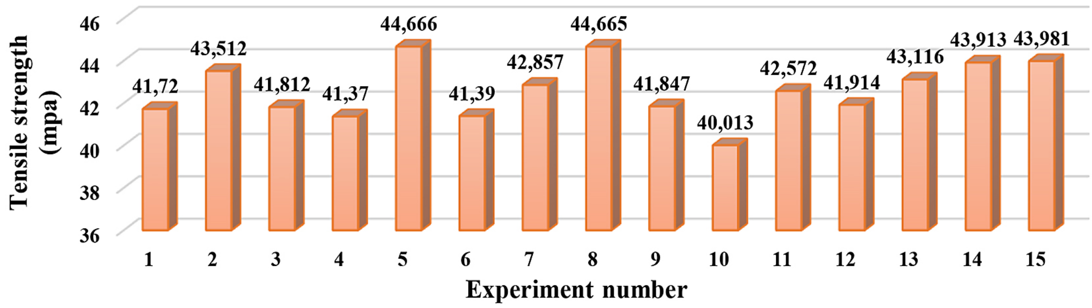

Figure 4. Tensile strength of PETG printed specimens

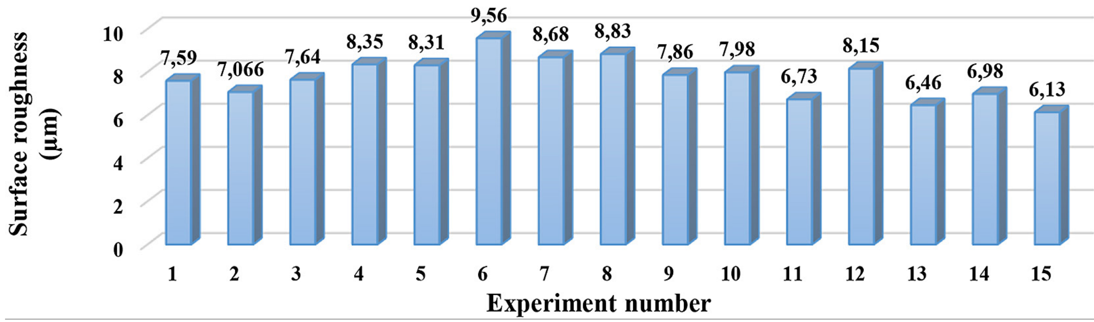

Figure 5. Surface roughness of PETG printed specimens

produces minimal impact on tensile strength because it demonstrates low result variability.

Infill density stands as the parameter that influences tensile strength the least based on the findings, while layer height and plate temperature showcase the strongest effects according to the Pareto chart. Improving the mechanical performance of 3D-printed components depends heavily on proper optimization of layer height and plate temperature, according to these experimental outcomes.

Figure 7 demonstrates that surface roughness depends mostly on infill density because roughness substantially reduces while infill density rises from 60% to 80%. Infill density plays an important role in improving the surface quality of 3D-printed parts, according to the results. Surface deformation and shrinkage increase as infill densities decrease because FDM prototypes have more voids, which results in higher roughness. The effect of plate temperature on surface roughness turns out to be moderately negative through the temperature range from 50 °C to 55 °C. The reduction in thermal non-uniformities and extrusion variations seems to explain the better results at higher build temperatures. The influence of layer height on surface roughness remains inconsistent because it displays minimal detectable traces.

The Pareto chart confirms that infill density stands as the top influencing factor for surface roughness, while plate temperature comes second, with layer height showing the least impact. The quantitative assessment using percentage breakdowns helps explain how each parameter affects total measurement variations. Layer height as an element produced the highest contribution rate to tensile strength measurements, amounting to 80.9% at a 95% confidence level, and infill density became the primary factor for surface roughness, with a 78% contribution. The table in Figure 6 presents the significance levels and optimal values for each factor that influences final results while showing the paramount importance of parameters in performance outcomes (Table 6).

Tensile strength and surface roughness relations are illustrated in Figures 8 and 9 through interaction graphs. The graphs show how different levels of a secondary variable influence connections between the primary factor and continuous measurement results. Each line depicts a different parameter level, while a mean scale represents the levels of the secondary parameter. These non-parallel lines in the graphs reflect important synergistic effects of FDM process parameters, which influence the overall characteristics of test specimens together.

Table 5. Analysis of variance results for tensile strength and surface roughness

ANOVA for tensile strength						
Source	DF	Adj SS	Adj MS	F-Value	P-Value	Percentage contribution
Model	9	23.7732	2.6415	8.02	0.017	93.52
Linear	3	4.6754	1.5585	4.73	0.064	18.4
A	1	0.0017	0.0017	0.01	0.945	0.006
B	1	20.5790	20.5790	7.83	0.038	80.9
C	1	20.0947	20.0947	6.36	0.053	79
Square	3	11.0443	3.6814	11.17	0.012	43.47
A*A	1	0.0537	0.0537	0.16	0.703	0.21
B*B	1	10.5093	10.5093	31.90	0.002	41.34
C*C	1	0.5802	0.5802	1.76	0.242	2.3
2-Way interaction	3	8.0535	2.6845	8.15	0.023	31.7
A*B	1	1.2476	1.2476	3.79	0.109	4.9
A*C	1	6.4602	6.4602	19.61	0.007	25.4
B*C	1	0.3458	0.3458	1.05	0.353	1.4
Error	5	1.6473	0.3295			6.5
Lack-of-Fit	3	1.1846	0.3949	1.71	0.390	4.6
Pure error	2	0.4627	0.2313			1.82
Total	14	25.4206				100
ANOVA for surface roughness						
Source	DF	Adj SS	Adj MS	F-Value	P-Value	Percentage contribution
Model	9	13.0903	1.45447	14.70	0.004	96.36
Linear	3	2.8577	0.95257	9.63	0.016	21.03
A	1	10.6074	10.60742	16.24	0.010	78
B	1	10.0325	10.03248	10.43	0.023	73.8
C	1	0.2178	0.21780	2.20	0.198	1.6
Square	3	9.3609	3.12029	31.53	0.001	68.9
A*A	1	4.8965	4.89653	49.48	0.001	36
B*B	1	0.0007	0.00066	0.01	0.938	0.005
C*C	1	5.0551	5.05512	51.08	0.001	37.22
2-Way interaction	3	0.8717	0.29056	2.94	0.138	6.41
A*B	1	0.1467	0.14669	1.48	0.278	1.1
A*C	1	0.3025	0.30250	3.06	0.141	2.22
B*C	1	0.4225	0.42250	4.27	0.094	3.1
Error	5	0.4948	0.09896			3.6
Lack-of-Fit	3	0.1275	0.04251	0.23	0.869	0.94
Pure error	2	0.3673	0.18363			2.7
Total	14	13.585				100

Note: DF denotes degrees of freedom, Adj SS represents the adjusted sum of squares, and Adj MS stands for the adjusted mean squares.

As explained in Figure 8, The best tensile strength for 3D-printed parts emerges when the device operates at 0.20 mm layer height with 45 °C plate temperature while maintaining 40% infill density. Figure 9 shows that material surface roughness reaches its minimum when the system operates with a combination of 60% infill density, which is linked to 50 °C temperature, coupled with a 0.20 mm layer height. The obtained data shows that determining interactive effects between factors remains vital for optimizing both mechanical performance and surface quality of

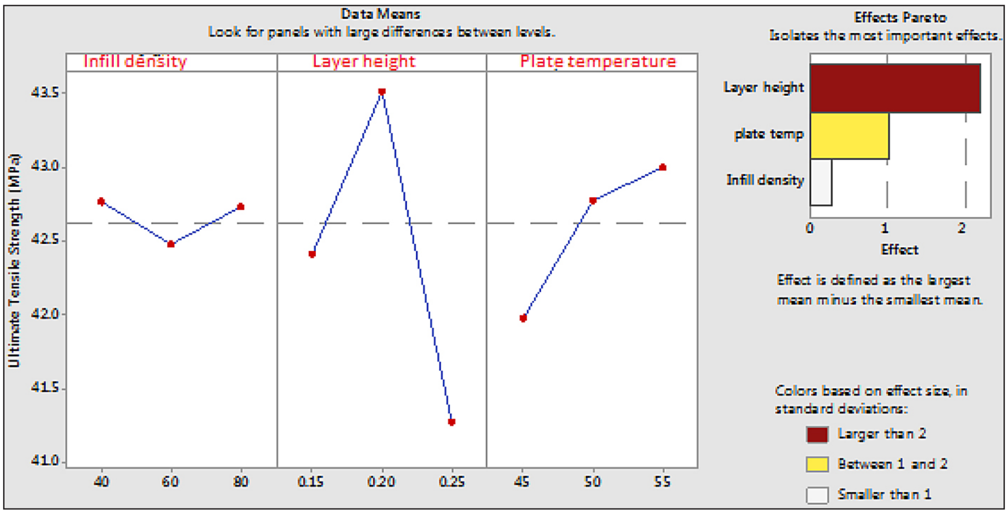

Figure 6. The main effects screener for tensile strength

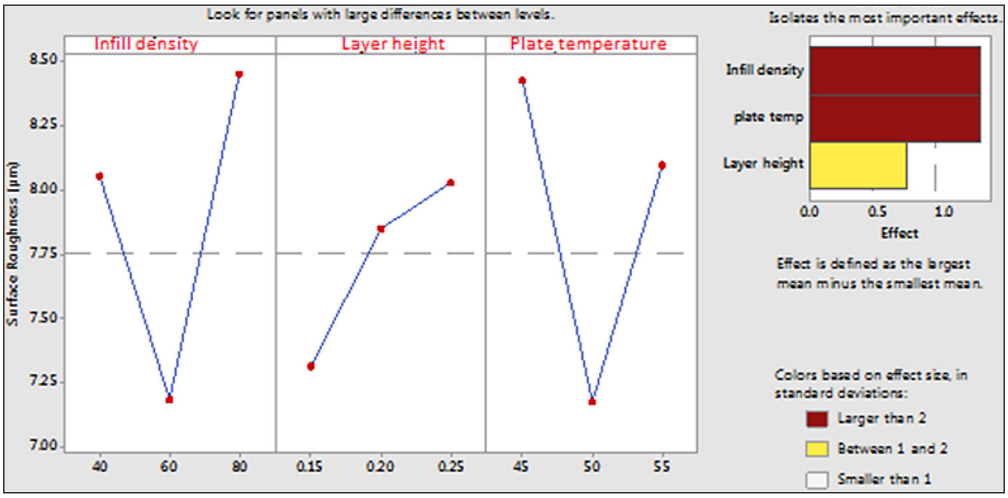

Figure 7. The main effect screener for surface roughness

Table 6. The significance and ideal values for every parameter

Parameters	Infill density %	Layer height (mm)	Plate Temperature (°C)	Significant
Optimized tensile strength	40	0.20	45	Layer height
Optimized surface roughness	60	0.20	50	Infill density

parts made through 3D printing. Can achieve high-quality final printed parts by controlling system parameters, leading to improved print results.

Equations 2 and 3 provide quadratic mathematical models that model the interactions between input variables and both tensile strength and surface roughness responses. These mathematical expressions evaluate total response effects by using linear and quadratic expressions with interaction terms. Mathematical equations function as predictive and optimization tools to explain extended knowledge about system outcomes affected by parameter interactions and individual parameters.

$$Tensile\ Strength\ (\text{MPa}) =$$
$$= -1.6 - 0.815 \times A + 209.8 \times$$
$$\times B + 1.32 \times C + 0.000301 \times A^2 - \quad (2)$$
$$-675 \times B^2 - 00159 \times C^2 - 0558 \times$$
$$\times A \times B + 001271 \times A \times C + 118 \times B \times$$

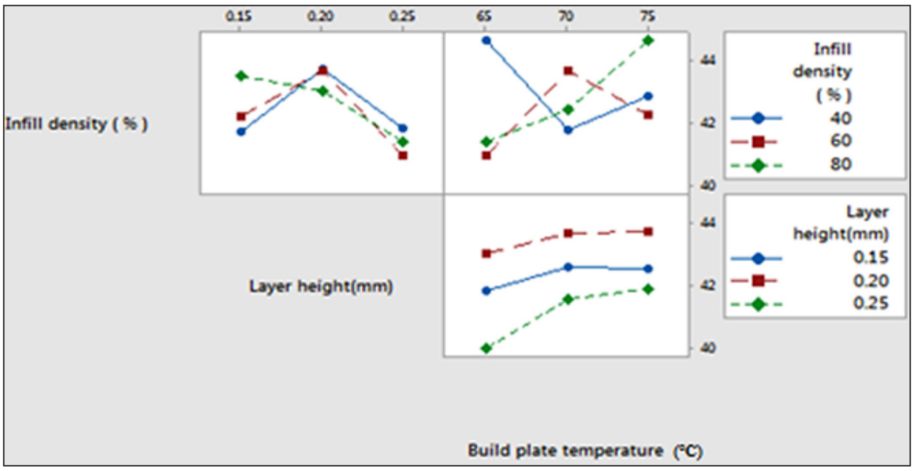

Figure 8. Tensile strength's interaction plot

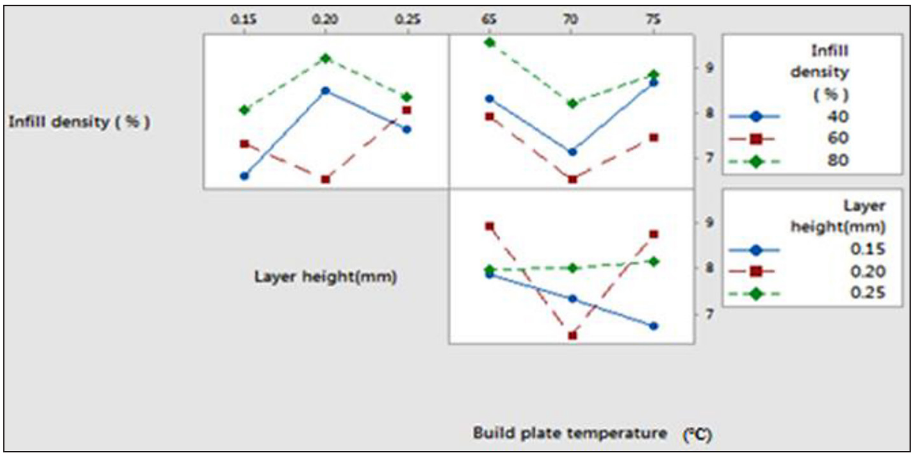

Figure 9. Surface roughness interaction plot

$$Surface\ Roughness\ (\mu m) = 256.6 - 0.205 \times A - 100.2 \times B - 6.68 \times C + 0.002879 \times A^2 - 5.4 \times B^2 + 0.04680 \times C^2 - 0.309 \times A \times B - 0.00275 \times A \times C + 1.300 \times B \times C \quad (3)$$

Table 7 shows an evaluation of the experimental findings for PETG part tensile strength and surface roughness by the RSM model, which implements Equation 4. Information in Table 7 and Figures 10 and 11 demonstrates that the experimental and predicted value error amounts to 1.28% for tensile strength and 6.54% for surface roughness. The RSM model delivers reliable predictions regarding mechanical properties, together with surface roughness measurements for the manufactured PETG specimens, because of its low error percentage figures. Experimental and predicted data match closely, which demonstrates that RSM provides reliable modeling and performance forecasting for PETG parts.

$$Error\ \% = \left|\left(\frac{Measured\ value - Predicted\ value}{Measured\ value}\right)\right| \times 100 \quad (4)$$

Optimized results

Desirability analysis (DA) optimizes several factors by allocating each a desirability score between 0 and 1, depending on whether greater values are desired or smaller values. By joining individual scores, an overall desirability index is formed to choose the most preferable input values. Following this approach helps manage many different response factors and makes choices for optimal process improvements and product design.The desirability analysis, equipped with

Table 7. Experimental versus RSM values for surface roughness and tensile strength

No.	Tensile strength (MPa)	RSM predicted tensile strength (MPa)	% Error	Surface roughness (µm)	RSM predicted surface roughness	% Error
1	41.720	42.13	0.97	6.590	7.41	2.33
2	43.512	43.215	0.68	8.066	7.19	1.78
3	41.812	42.11	0.71	7.640	7.51	1.6
4	41.370	40.96	0.98	8.350	8.5	2.12
5	44.666	44.168	1.11	8.310	8.5	2.72
6	41.390	41.6	0.49	9.560	9.48	0.8
7	42.857	42.65	0.48	8.680	8.7	0.88
8	44.665	45.16	1.11	8.830	8.6	2.56
9	41.847	41.93	0.214	7.860	7.8	0.62
10	40.013	40.21	0.49	7.980	7.87	1.26
11	42.572	42.37	0.47	6.730	6.83	1.49
12	41.914	41.85	0.213	8.150	8.19	0.604
13	43.116	43.67	1.28	6.460	6.52	0.98
14	43.913	43.67	0.55	6.980	6.52	6.54
15	43.981	43.67	0.71	6.130	6.52	6.42

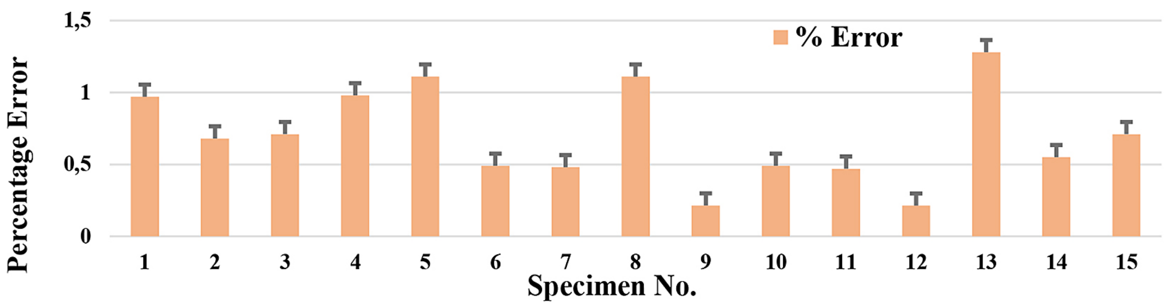

Figure 10. Comparison using the percentage error between the experimental and predicted tensile strength

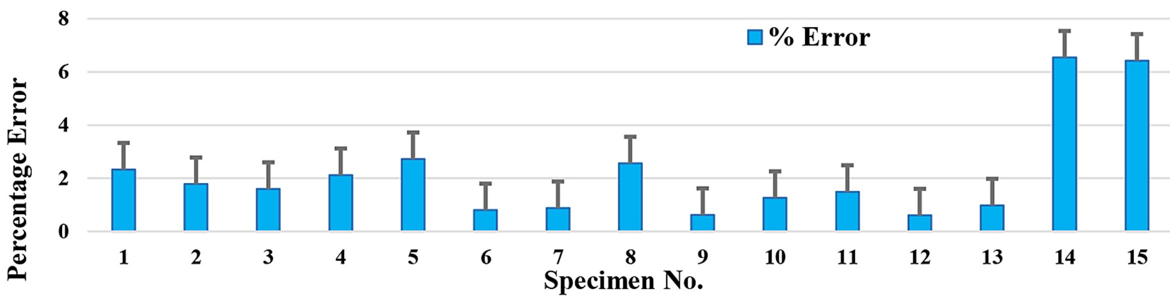

Figure 11. Comparison using the percentage error between the experimental and predicted surface roughness

a response optimizer, optimized both tensile strength and surface roughness performance as part of the RSM framework. The optimization results displayed in Figure 12 illustrate how the desirability value reached 0.8645 and signifies the achievement of an appropriate conflicting requirement balance. A set of optimal inputs for the 3D printer consisted of 64.24% infill density while also needing 0.1813 mm layer height alongside 51.46 °C plate temperature. Under these experimental conditions, the predicted tensile strength measurement reaches 43.85 MPa with an exceptional desirability outcome of 0.825. The surface roughness optimization reached 6.45 µm when the essential parameters produced a desirability value of 0.904. This indicates moderate optimization. Surface roughness expands simultaneously as both infill density and plate temperature

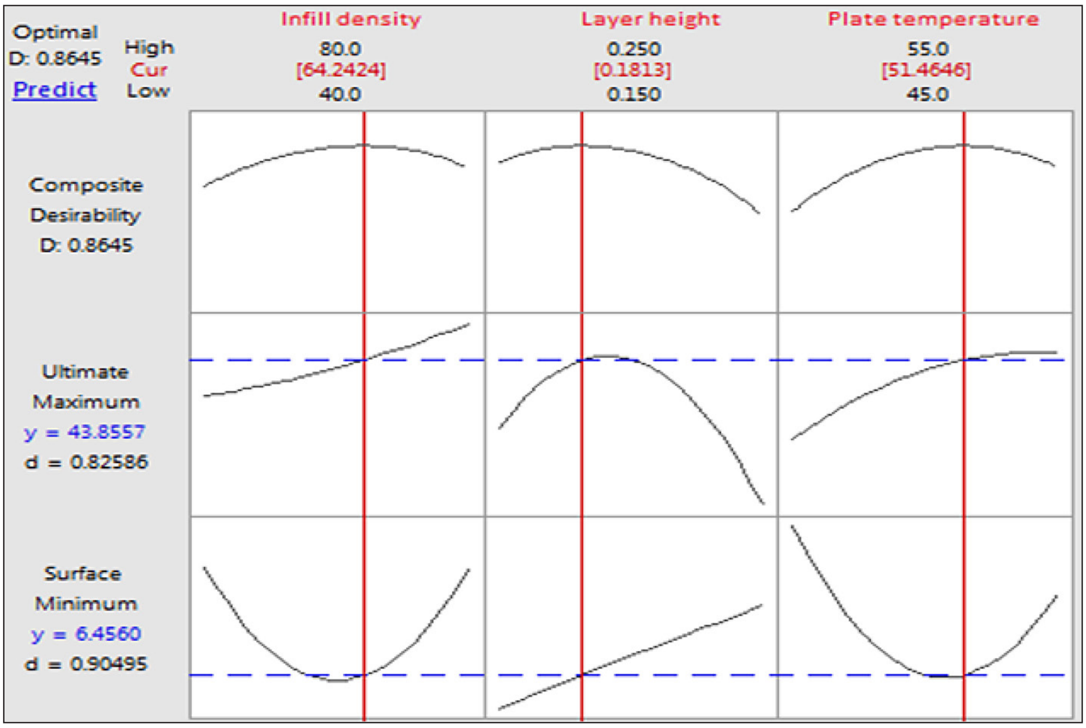

Figure 12. Optimization of tensile strength and surface roughness

increase, yet higher layer height results in decreasing tensile strength. By effectively handling conflicting factors, the selected parameter set achieves both improved mechanical strength and satisfactory surface roughness.

CONCLUSIONS

This study focused on achieving optimal FDM process settings for PETG material to enhance roughness quality while increasing tensile strength performance. The creation of predictive models to link observed responses with important process parameters was accomplished through a Box–Behnken design operating within the framework of response surface methodology. The investigation produced important outcomes that are summarized as follows:

- The best tensile strength measurement resulted from using 40% infill density with 0.2 mm layer height at 45°C plate temperature.
- With an infill density of 60%, a layer height of 0.2 mm, and a plate temperature of 50 °C, the minimum surface roughness was achieved at 6.13 µm.
- Tensile strength variations were primarily explained through the changes in layer height among all tested parameters, with a contribution of 80.9%. Surface roughness demonstrated the highest dependence on infill density since this factor accounted for 78% of the total variation.
- It was discovered through desirability analysis that the best values for maximum tensile strength and smooth surface were 64.24% infill density, a layer height of 0.1813 mm, and a plate temperature of 51.46 °C. This configuration enhances the support of functional applications that require mechanical durability and accuracy.
- Tensile strength and roughness values were predicted with limited errors, with predictive models showing high accuracy at 1.28% for tensile strength and 6.54% for roughness. This confirms that RSM helps optimize both PETG for aerospace brackets and for automotive prototype parts.

The study established through their study that RSM successfully identifies optimal FDM processing parameter sets for PETG to create improved mechanical and surface geometrical components. Research expansion for the future should focus on including infill patterns together with print speed and composite materials as additional factors to enhance FDM process flexibility for aerospace, automotive, and bioengineering applications.

REFERENCES

1. Cao L, Xiao J, Kim JK, Zhang X. Effect of post-process treatments on mechanical properties and surface characteristics of 3D printed short glass fiber reinforced PLA/TPU using the FDM process. CIRP Journal of Manufacturing Science and Technology. 2023 Apr 1; 41:135–43. https://doi.org/10.1016/j.cirpj.2022.12.008
2. Khan I, Barsoum I, Abas M, Al Rashid A, Koç M, Tariq M. A review of extrusion-based additive manufacturing of multi-materials-based polymeric laminated structures. Composite Structures. 2024 Aug 21:118490. https://doi.org/10.1016/j.compstruct.2024.118490
3. Mansor KK, Shabeeb AH, Hussein EA, Abbas TF, Bedan AS. A Statistical investigation and prediction of the effect of FDM variables on flexural stress of PLA prints. Tikrit Journal of Engineering Sciences. 2024 Jul 2; 31(3):10–7. https://doi.org/10.25130/tjes.31.3.2
4. Al-Bdairy, AMJ, Ghazi SK, and Abed AH. Prediction of the mechanical properties for 3D printed rapid prototypes based on artificial neural network. Advances in Science and Technology. Research Journal 2025; 19(3): 96–107.
5. Al-Duroobi, AAA, Al-Bdairy AM, and Al-Juboori L. Rapid prototyping of sculpture surfaces based on discrete algorithm using 3D printer technique. 2024 Advances in Science and Engineering Technology International Conferences (ASET). IEEE, 2024.
6. Sani AR, Zolfagharian A, Kouzani AZ. Artificial intelligence-augmented additive manufacturing: insights on closed-loop 3D printing. Advanced Intelligent Systems. 2024 Oct;6(10):2400102. https://doi.org/10.1002/aisy.202400102
7. Samykano M, Kumaresan R, Kananathan J, Kadirgama K, Pandey AK. An overview of fused filament fabrication technology and the advancement in PLA-biocomposites. The International Journal of Advanced Manufacturing Technology. 2024 May; 132(1):27-62. https://doi.org/10.1007/s00170-024-13394-1
8. Frunzaverde D, Cojocaru V, Bacescu N, Ciubotariu CR, Miclosina CO, Turiac RR, Marginean G. The influence of the layer height and the filament color on the dimensional accuracy and the tensile strength of FDM-printed PLA specimens. Polymers. 2023 May 19; 15(10):2377. https://doi.org/10.3390/polym15102377
9. Sudin MN, Shamsudin SA, Daud NM, Yusuff MA. Examining the effect of annealing parameters on surface quality and tensile strength of ABS 3D-printed materials. El-Cezeri. 2024 Jan 9; 11(3):307–16. https://doi.org/ 10.31202/ecjse.1369831
10. Farashi S, Vafaee F. Effect of printing parameters on the tensile strength of FDM 3D samples: a meta-analysis focusing on layer thickness and sample orientation. Progress in Additive Manufacturing. 2022 Jan 16:1–8. https://doi.org/10.1007/s40964-021-00247-6
11. Lalegani Dezaki M, Ariffin MK, Serjouei A, Zolfagharian A, Hatami S, Bodaghi M. Influence of infill patterns generated by CAD and FDM 3D printer on surface roughness and tensile strength properties. Applied Sciences. 2021 Aug 7; 11(16):7272. https://doi.org/10.3390/app11167272
12. Shirmohammadi M, Goushchi SJ, Keshtiban PM. Optimization of 3D printing process parameters to minimize surface roughness with hybrid artificial neural network model and particle swarm algorithm. Progress in Additive Manufacturing. 2021 May; 6:199–215. https://doi.org/10.1007/s40964-021-00166-6
13. Mat MA, Ramli FR, Sudin MN, Herawan SG, Alkahari MR. The effect of tensile strength and surface roughness by varying oxygen level in 3D printer chamber. J. Tribol. 2022; 33:80–96.
14. Mani M, Karthikeyan AG, Kalaiselvan K, Muthusamy P, Muruganandhan P. Optimization of FDM 3-D printer process parameters for surface roughness and mechanical properties using PLA material. Materials Today: Proceedings. 2022 Jan 1; 66:1926–31. https://doi.org/10.1016/j.matpr.2022.05.422
15. Abdulridha HH, Abbas TF. Analysis and investigation the effect of the printing parameters on the mechanical and physical properties of PLA parts fabricated via FDM printing. Advances in Science and Technology. Research Journal. 2023; 17(6). http://dx.doi.org/10.12913/22998624/173562
16. Fadillah F, Suryanto H, Suprayitno S. Study on effect of 3D printing parameters on surface roughness and tensile strength using analysis of variance. Journal of Mechanical Engineering Science and Technology (JMEST). 2023; 7(2):96.
17. Hamat S, Ishak MR, Sapuan SM, Yidris N, Hussin MS, Abd Manan MS. Influence of filament fabrication parameter on tensile strength and filament size of 3D printing PLA-3D850. Materials Today: Proceedings. 2023 Jan 1; 74:457–61. https://doi.org/10.1016/j.matpr.2022.11.145
18. Kónya G. Investigating the impact of productivity on surface roughness and dimensional accuracy in FDM 3D printing. Periodica Polytechnica Transportation Engineering. 2024 Feb 12; 52(2):128–33. https://doi.org/10.3311/PPtr.22952
19. Özkül M, Kuncan F, Ulkir O. Predicting mechanical properties of FDM-produced parts using machine learning approaches. Journal of Applied Polymer Science. 2025:e56899. https://doi.org/10.1002/app.56899
20. Abdullah MA, et al. Comparison between low-carbon steel and galvanized steel by deep drawing under the influence of different parameters. Management

Systems in Production Engineering, 2025; 33(2):163–170. https://doi.org/10.2478/mspe-2025-0016

21. Mohsein ZH, Abdulwahhab AB, Abbas A. Study effect of active flux on mechanical properties of TIG welding process, Results in Engineering 2025; 26: 104681. https://doi.org/10.1016/j.rineng.2025.104681
22. Mohammed, AR, and Jawad WK. Practical test and FEA to evaluation of the thickness distribution for octagonal cup generated by deep drawing. AIP Conference Proceedings. 2024; 1:3002. AIP Publishing,
23. Ghazi SK., Abdullah MA and Abdulridha HH. Investigating the impact of EDM parameters on surface roughness and electrode wear rate in 7024 aluminum alloy. Engineering, Technology & Applied Science Research. Feb. 2025; 15(1):19401–19407. https://doi.org/10.48084/etasr.9252
24. Abdullah MA, Ahmed BA and Ghazi SK. 2024. Enhancing of material removal rate and surface roughness in wire EDM process using grey relational analysis. Engineering, Technology & Applied Science Research. Oct. 2024; 14(5):17422–17427. https://doi.org/10.48084/etasr.8450
25. Abdullah MA, Abbas TF. Numerical developing the internet of things to remotely monitor the performance of a three dimensions printer for free-form surface. Journal of Engineering Science and Technology. 2023 Dec; 18(6):2809–22.